

SAMARRA JOURNAL OF ENGINEERING SCIENCE AND RESEARCH



Experimental study of the effect of nanomaterials on the thermal, magnetic, and corrosion properties of aluminium and copper tubes in solar collector system

Mhmood Shakir Kadhim AL Hamrah

Najaf water directorate, Najaf, Iraq

Article Information

Received: 25/4/2025 Accepted: 20/7/2025

Keywords

Corrosion effect, Solar Collector, Magnetic, Nanofluids, Aluminium- copper tubes.

Corresponding Author

E-mail:

mahmoodkied3@gmail.com

Abstract

Solar collectors are currently widely used to harness solar energy in various applications to achieve sustainable development goals. Solar collectors suffer from persistent corrosion of copper and aluminium tubes due to exposure to air and oxidation. Also the increasing of the thermal conductivity of the fluids using highly conductive nanomaterials. This investigation examined the effect of the utilization of magnetic fluids on the corrosion of flat plate collectors made of aluminium and copper. The outcomes of thermal conductivity tests indicated that the thermal conductivity of graphene-based nano fluids was 23.1% greater than the thermal conductivity of water (concentrated of 0.1%vol., temperature 50 °C). The thermal conductivity of the nanofluids containing carbon nanotubes was also increased by 33.44% compared to the water thermal conductivity (0.1% vol. temperature 50 °C). The outcomes of the solar collector's tube corrosion experiments demonstrated that the corrosion potentials of aluminium samples in base fluid, G+Fe₃O₄ nanofluid and CNT+ Fe₃O₄ nanofluid were all negative, which were: 0.95, 0.85 and 0.84, respectively. This demonstrates that the corrosion resistance of aluminium tubes in solar collectors in G+ Fe₃O₄ and CNT+ Fe₃O₄ fluid samples was enhanced by 14.32% and 15.03%, respectively, compared to water. The corrosion potentials of copper samples in base fluid, G+ Fe₃O₄ nanofluid and CNT+ Fe₃O₄ nanofluid are -0.82679, 0.77224 and 0.77058, respectively. This implies that the corrosion resistance of solar collectors made of copper in G+ Fe₃O₄ and CNT+ Fe₃O₄ is increased by 6.598% and 6.799%, respectively, compared to water.

1. Introduction

Nano fluids have unique properties that make them a cornerstone in the design and implementation of solar collectors. Nano fluids are prepared by mixing and dispersing nanomaterials in a certain amount of fluid, forming a new type of fluid with great potential for practical industrial applications. The particle sizes used in nano fluids range from 1 nm to 100 nm [1-3]. Some researchers have studied the effect of adding micro particles to a fluid in appropriate quantities; however, they found that they lack the necessary stability in suspended form and observed rapid sedimentation of these particles to the bottom of the solar collector basin. This sedimentation can quickly slow fluid flow. Conversely, nanoparticles have higher stability in suspended form, and their low sedimentation rate reduces the problem of channel clogging [4-6]. Nano fluids have superior thermal and optical properties and can also directly increase sunlight absorption. Nano fluids derived from conventional methods have low colloidal stability, and in contrast, single-step methods are more expensive. Consequently, it is crucial to create nano fluids using a cost-effective, one-step method [7-10]. The combination of multiwalled carbon nanotubes and magnetic materials offers multiple and interesting properties for each component and opens up new opportunities for a variety of practical applications. Several different fabrication methods have been used in the past to create magnetite-based carbon nanotubes [8-12]. The basic principle of a flat-plate solar collector is simple: sunlight is absorbed through a transparent coating and covered with an absorber layer. The absorber captures a significant portion of the solar radiation energy, which is converted into energy and transmitted to the fluid in the channel [12-15]. Thus, the cold fluid from the lower collector inlet is heated by solar energy in the fluid path, causing the temperature to rise over time. The heated medium carries the available thermal energy from the top of the collector to the storage area. In addition, as the absorber temperature rises, the heat is released to the environment through the transparent coating and shell, resulting in a variety of heat losses in the flat-plate collector [16-18]. Due to the poor thermal properties of the working fluid, the flat-plate collector is primarily responsible for the majority of the stored heat, and this loss is exacerbated by the fact that the collector is located in a greenhouse [19,20]. In a study by Sun et al., the effect of a static magnetic field on the convective heat transfer of a magnetite-based aqueous nanofluid in horizontal circular tubes was observed [21]. Choi et al. studied the heat transfer and flow characteristics of a magnetite-based aqueous nanofluid in the presence of a magnetic field and evaluated it experimentally [22]. In a study by Batad et al., they investigated the characterization of magnetic iron oxide-based nanofluids for thermal treatment. Iron oxide (Fe₂O₃) nanoparticles were produced by solution coagulation and spontaneous combustion. The structure, morphology, and properties of the resulting zinc nanoparticles were evaluated using X-ray diffraction (XRD), fieldemission scanning electron microscopy (FE-SEM), and a vibrating probe magnetometer [23]. Hussain et al. studied magnetic nanofluids based on multi-walled carbon nanotubes with magnetite nanoparticles for heat transfer applications, and documented the creation of magnetite nanoparticles and carbon nanotubes for heat transfer [24]. Jang et al. studied the effects of using magnetic fluids in planar solar collectors. The variables examined were: changing the working fluid, changing the working fluid concentration, changing the corrosion effect, and changing the tube [25]. Raki et al. determined the final formulation by observing changes in the corrosion rate and fitting the laboratory data to a corrosion rate curve to achieve the optimal nano fluid concentration [26]. Abdeen et al. presented experiments evaluating the corrosion potential of magnetic nano fluids in the laboratory, followed by experiments evaluating the corrosion potential of carbon-based magnetic nano fluid. In addition, a new methodology is being followed to maximize the efficiency of nano fluid concentrations. The thermal performance is determined in the same way, and the efficiency of the two nano fluids is evaluated in terms of overall efficiency. [27]

Previous studies have not investigated the effects of magnetic nano fluids and the addition of carbon nanotubes to flat-plate solar collectors. No similar studies have been conducted on the effects of different nano fluids on the corrosion of aluminium and copper tubes used in flat-plate collectors. Similarly, no studies have been conducted on the effects of magnetic fluids on the corrosion of aluminium and copper tubes in flat-plate collectors, nor have any studies been conducted on the effects of carbon fluids on the corrosion of aluminium and copper tubes in flat-plate collectors. Furthermore, no comparison has been made between the effects of magnetic nano fluids and the addition of carbon nanotubes to aluminium or copper solar collectors. Furthermore, the concentration of nano fluids was not specifically designed to reduce costs. The effect of reducing corrosion on the repair and maintenance costs of flat-plate collectors has not been documented. It has previously been reported that the use of magnetic fluids alters the corrosion of aluminium and copper tubes in flat-plate solar collectors, and that replacing them would increase their maintenance costs. Consequently, these tubes must be replaced after a certain period of time. This research aims to achieve several objectives:

The first objective of this research includes studying the corrosion of aluminium and copper sheets using two different nano fluids: magnetic nano fluids and a mixture of magnetic and carbon nano fluids.

The second objective is to prevent the corrosion of aluminium and copper tubes, which will in turn reduce the maintenance cost of flat-plate solar collectors. Materials and Methods. This research aims to prepare aqueous nano fluids such as Fe_3O_4 , carbon nanotubes, and graphene, as well as nano fluids from a mixture of nanomaterials.

The final objective includes studying the thermal, structural, and magnetic properties of the prepared Nano fluids and their effect on the heat transfer coefficient and corrosion of copper and aluminium tubes in the solar collector.

2. Experimental work

2.1 Nano fluid preparation

The most significant component of measuring the thermos physical properties of nanofluids is the preparation of the fluid. In this research, different concentrations of carbon nanoparticles were incorporated into a specific volume of distilled water. To maximize the dispersal of carbon nanoparticles in water-based media, a pH meter, magnetic stirrer, and ultrasound were employed. After 60 min of magnetic stirring, the suspensions with a mass fraction of 0.2, 0.4, 0.6, 0.8, and 1.0%/mL (which is equal to 1% of carbon particles mixed with 100 cm³ of water) were stirred for 40 min using a 400 W, 24 kHz ultrasonic processor (Hilscher, Germany). These devices

were employed to dissociate clusters of nanoparticles and produce consistent dispersions. Fig. 1 depicts a depiction of the carbon nanoparticles employed. Fig. 1 illustrates the makeup of the carbon nanoparticles and the liquid before and after being ultra-sonicated.

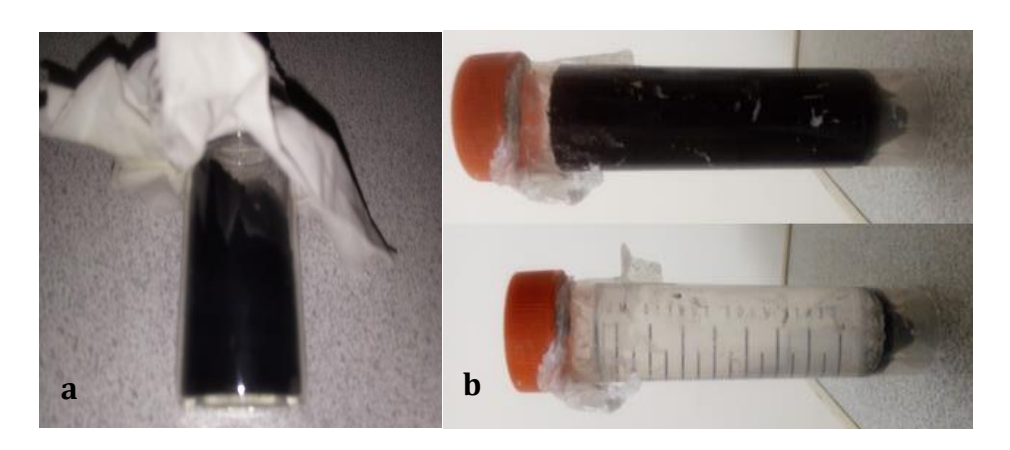


Fig. 1. (a) Carbon nanoparticles (b) Combination of fluid and carbon nanoparticles before and after ultrasonic.

2.2 Substrate and its preparation

In this research, aluminum pipe with thicknesses of 1.0, 1.5 and 1.6 mm and copper pipe of 12.7 mm with thicknesses of 0.63, 0.75 and 0.81 were used.

To prepare the surface of the substrate, first sanding operations were performed on the desired samples with SiC sandpaper with numbers 360, 400, and 600 respectively. Next, degreasing and cleaning of the samples were done in acetone, alcohol and distilled water environments, each for 20 minutes, using an ultrasonic bath (SB-5200D, made by Scientz, China). After that, the samples were dried with hot air pressure and kept in a desiccator until the corrosion test operation.

2.3 Methods

The phase composition of the nanoparticles was determined by X-ray diffraction (XRD-D8ADVANCE, Bruker). The diffraction patterns were recorded using a Cu-K α lamp with a wavelength of λ = 1.541 Å in the range of 800>2Ø>10, at a step size of 0.05 and a step length of 1 s. Phase detection was performed using standard maps and the information provided in the X'Pert software.

The functional groups of the nanoparticles were characterized by Fourier transform infrared spectroscopy (FTIR-JASCO 6300JAPAN). The spectral patterns were recorded in the range of 400–4000 (/cm) with a scanning speed (resolution accuracy) of 4/cm. The functional groups and their relative values were determined by comparing the infrared spectra and the intensities of the spectral peaks with the information in the standard table (IRPal software).

The microstructure (morphology and homogeneity) of the nanoparticles was studied using a field emission scanning electron microscope (FESEM-NOVA-HV) at an operating voltage of 10 kV. A very thin layer of gold was deposited on the samples using a physical vapor deposition and diffusion coating equipment (DST3-T, produced by Nanostructured Coatings).

The heat transfer of the nanofluids was measured using a KD2 Pro thermal performance analyzer (Decagon Devices, Inc., USA) with an error of 5%. The KD2 Pro uses the hot wire method. The heat transfer of the nano fluids was measured using a single pin sensor KD2 Pro KS-1 (stainless steel). The single pin sensor was immersed in the nano fluid in a temperature bath. The KD2 Pro was calibrated with pure water before the test and the results were compared with the available heat transfer data for distilled water. Three heat transfer measurements were performed at temperatures of 25, 30, 35, 40, 45, and 50 °C. To verify the thermal conductivity of the nano fluid samples, thermal conductivity tests were performed using a heat transfer device (KD2 Pro) at a temperature rate of 20 to 50 °C in steps of 5 °C.

There are some benefits of Carbon nanotubes compared with Graphene platelets which make it an ideal choice due to their unique properties:

- High strength-to-weight ratio: Carbon nanotubes are known to be the strongest and stiffest materials in terms of tensile strength and elastic modulus.
- One-dimensional (1D) structures: Their tubular structure allows for unique applications in solar collectors, where they act as a good thermal conductor when carbon nanotubes are mixed with fluids.
- Light weight: which allows them to spread smoothly in fluids and prevent them from clumping or settling at the bottom of the solar collector basin.
- Due to their cylindrical shape, carbon nanotubes have a high flow rate compared to flat graphene sheets, which can impede the movement of the nano fluid.
- Smooth texture, which prevents them from sticking to the walls of the tubes used in solar collectors compared to graphene nano platelets.

3. Results and discussion

3.1 XRD characterization

In Fig. 2 the X-ray diffraction pattern for Fe_3O_4 magnetic nanoparticles can be seen. Fe_3O_4 magnetic nanoparticles have a characteristic peak at 2Θ =30.277° with an interlayer distance of 2.9496 angstroms, 2Θ =35.582° with an interlayer distance of 2.5211 angstroms and 2Θ =43.124° with an interlayer distance of 2.0960. It is Angstrom.

In Fig. 2, the X-ray diffraction pattern for carbon nanotubes and composite carbon nanotubes/ Fe304 magnetic nanoparticles can be seen. The carbon nanotube has a characteristic peak at 2θ =26.041° with an interlayer distance of 3.41 angstroms and 2θ =42.597° with an interlayer distance of 2.1207 angstroms. Also, the presence of peaks 2θ =26.373°, 2θ =30.277° and 2θ =35.578°, respectively with the interlayer distance of 3.3767, 2.9544 and 2.5213 Angstroms, which are characteristic peaks of carbon nanotubes and Fe304 magnetic nanoparticles, the combination of this They confirm two things.

In Fig. 2, the X-ray diffraction pattern for graphene carbon nanoparticles and graphene composite/ Fe_3O_4 magnetic nanoparticles can be seen. graphene carbon nanoparticles have a characteristic peak at 26.463° with an interlayer distance of 3.36 angstroms and 54.57° with an

interlayer distance of 1.68 angstroms. Also, the presence of peaks at 2θ =26.68°, and 2θ =35.68°, with an interlayer distance of 3.386 and 2.51 Angstroms, respectively, which are characteristic peaks of graphene carbon nanoparticles and Fe₃O₄ magnetic nanoparticles, confirm the composition of these two materials.

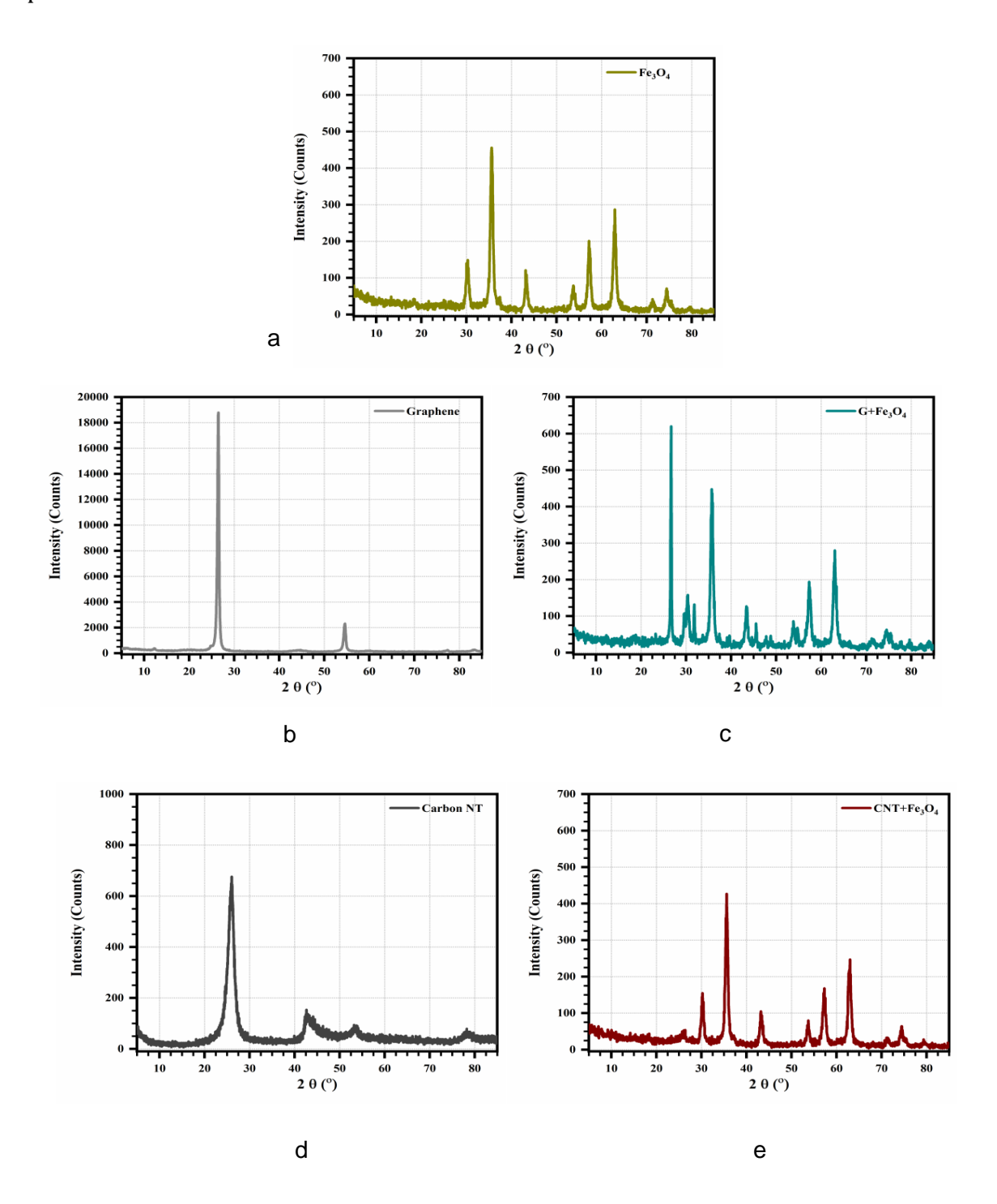


Fig. 2. X-ray diffraction pattern for (a) Fe_3O_4 magnetic nanoparticles, (b) Carbon nanotubes, (c)carbon nanotubes/ Fe_3O_4 magnetic nanoparticles, (d) Graphene carbon nanoparticles and (e) graphene/ Fe_3O_4 magnetic nanoparticles.

3.2 FTIR results

Fourier transform infrared spectroscopy was performed to determine the structure and functional groups of three materials: Fe₃O₄ magnetic nanoparticles, carbon nanotubes and graphene carbon nanoparticles as shown in Fig. 3. The goal of infrared absorption spectroscopy is to measure the highest absorption of light at different wavelengths. The simple way is to measure the amount of absorption by shining a monochromatic beam at a certain wavelength (monochromatic) to a sample and repeating it for other wavelengths. In the Fourier transform infrared spectrometer, instead of irradiating a single beam to the sample, a beam with thousands of different frequencies or wavelengths is irradiated to the sample at the same time and the amount of absorption and how it is analyzed. A peak with higher radiation intensity in the frequency (deeper peak) indicates the presence of a functional group with less ability to absorb light energy, while a peak with lower radiation intensity (higher absorption) means the presence of a functional group with a higher vibrational energy equivalent [13]. The peak between 3400 and 3600 (cm⁻¹) was shown in the spectrum pattern, which is related to (0-H). The peak between 1550 and 1610 (cm⁻¹) was shown in the spectrum pattern, which is related to (C-0). The peak between 1000 and 1350 (cm⁻¹) was shown in the spectrum pattern, which corresponds to (C-F). The peak between 600 and 700 (cm⁻¹) was shown in the spectrum pattern, which is related to (C-H).

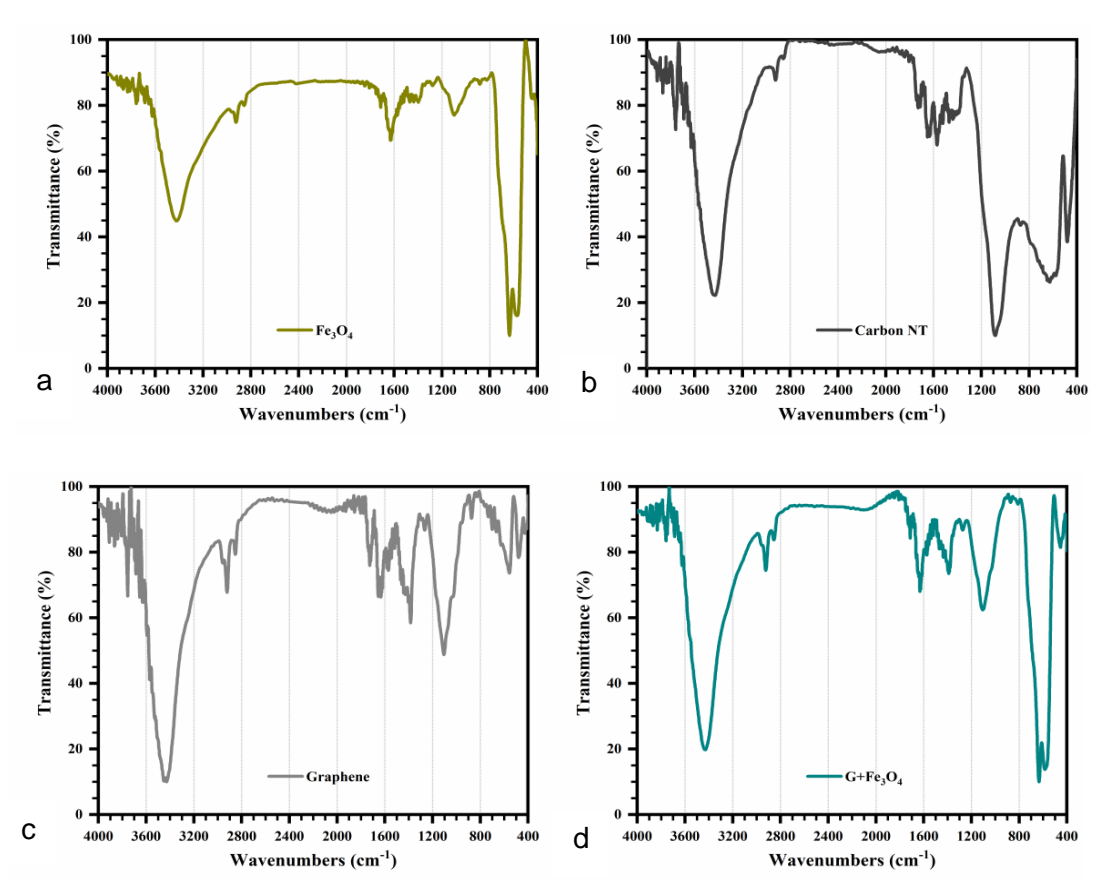


Fig. 3. Infrared spectrum pattern for (a) Fe_3O_4 magnetic nanoparticles, (b) Carbon nanotubes, (c) Graphene carbon nanoparticles and (d) graphene/ Fe_3O_4 magnetic nanoparticles.

3.3 SEM images results

The surface morphology of three materials, Fe_3O_4 magnetic nanoparticles, graphene carbon nanoparticles and composite graphene/ Fe_3O_4 magnetic nanoparticles, as well as carbon nanotubes as shown in Fig. 4. As can be seen, Fe_3O_4 magnetic nanoparticles have a zero-dimensional structure, which means that the particles have a spherical morphology. In addition, the particle size is below 100 nm, while for example carbon nanotube and graphene, it is one-dimensional and two-dimensional structure, respectively. Field emission scanning electron microscope images for the microstructure of the composite sample show a good dispersion of Fe_3O_4 magnetic nanoparticles in the graphene matrix, which are entangled and homogenized.

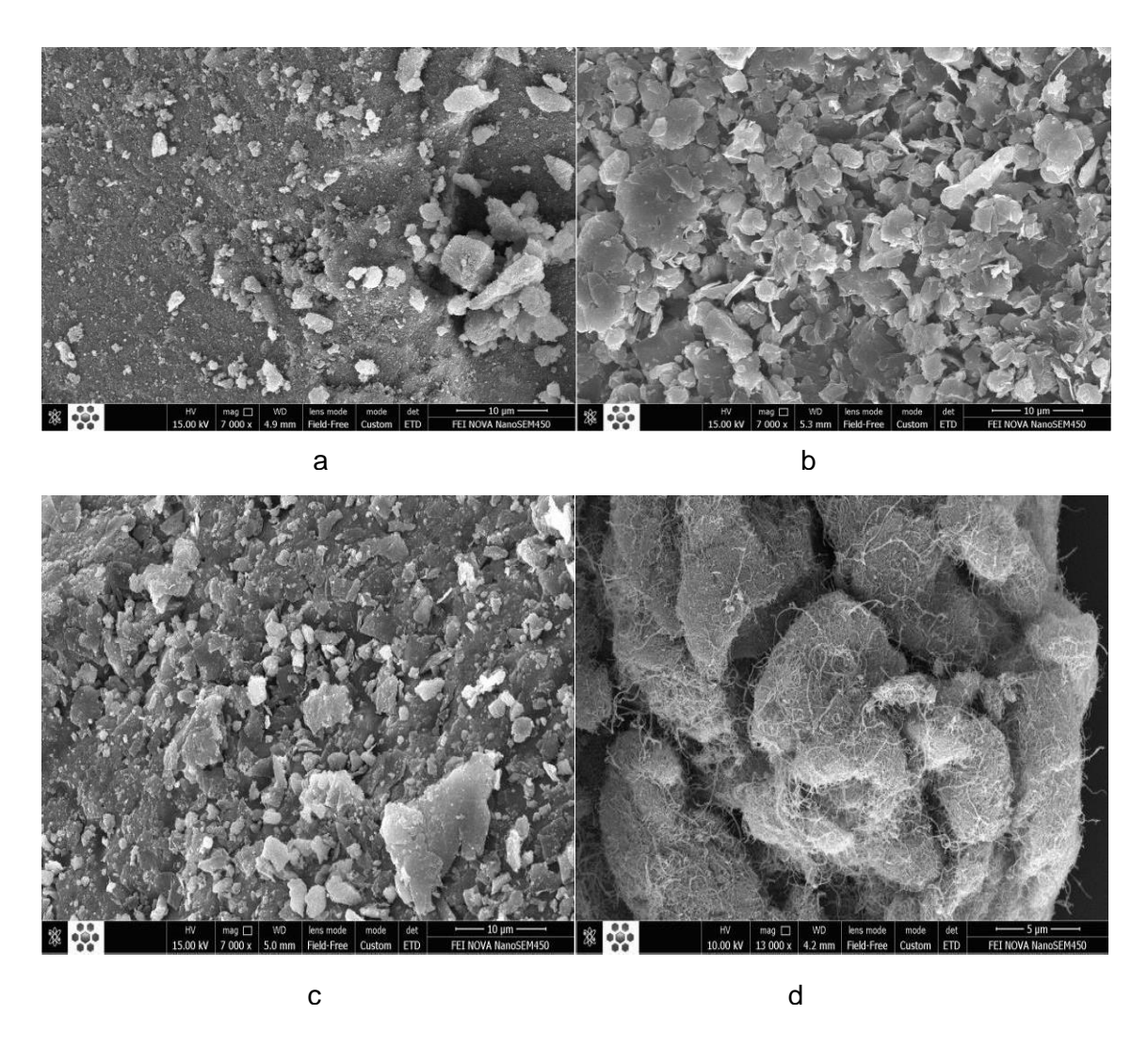


Fig. 4. FESEM images for (a) Fe₃O₄ magnetic nanoparticles, (b) Graphene carbon nanoparticles, (c)graphene/ Fe₃O₄ magnetic nanoparticles and (d) Carbon nanotubes.

3.4 Magnetometer test

The magneto metric test for magnetic nanoparticles in the composite is shown in Fig. 5 Sample A (CNT+ Fe₃O₄) has higher magnetization than sample B (G+ Fe₃O₄) because all the outer electrons of the carbon hex atomic rings in graphene are fully paired to form σ and π bonds.

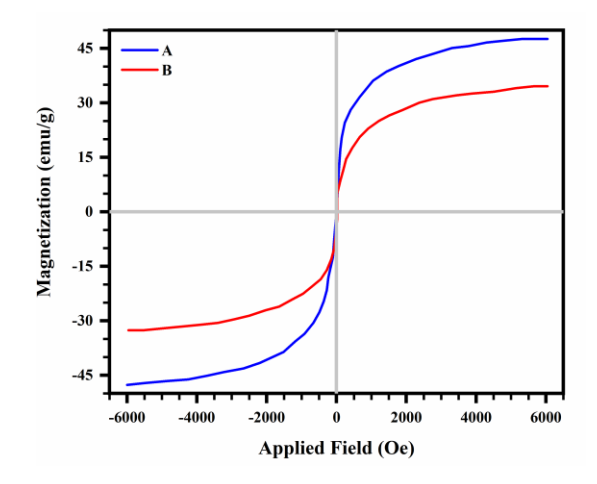


Fig. 5. Magneto metric test of magnetic nanoparticles in composite.

3.5 Corrosion test

The corrosion test for two composites, each for two copper and aluminum pipes, is performed in Fig. 6. The potentio dynamic polarization curves are shown for copper and aluminum tubes with different types of Nano fluids. From these curves, corrosion potential, corrosion current density, and anodic and cathodes Tafel constants can be extracted. The higher the TOEFL coefficient, the faster the polarization and the lower the corrosion rate. On the contrary, lower TOEFL leads to slower polarization and more corrosion. By knowing the values of the current density, the corrosion behavior of the samples can be evaluated. The lower the corrosion current density, the higher the polarization resistance and corrosion resistance of the pipe. The results of this study show that the lower thermal conductivity of nano fluid has a significant effect on reducing corrosion resistance. Also, the results show that adding solid nanoparticles to the base fluid and forming nano fluid has a great effect on improving corrosion resistance.

Corrosion potential for aluminum sample in base fluid, $G+ Fe_3O_4$ nano fluid and CNT+ Fe_3O_4 nano fluid is negative 0.99150, 0.84949 and 0.84247 respectively. which shows the improvement of the corrosion resistance of solar collector aluminum tube in $G+ Fe_3O_4$ nano fluid and CNT+ Fe_3O_4 nanofluid samples compared to water, equal to 14.32 and 15.03%, respectively.

Corrosion potential for copper sample in base fluid, $G+ Fe_3O_4$ nanofluid and CNT+ Fe_3O_4 nanofluid is negative 0.82679, 0.77224 and 0.77058 respectively. which shows the improvement of the corrosion resistance of solar collector copper tube in $G+ Fe_3O_4$ nanofluid and CNT+ Fe_3O_4 nanofluid samples compared to water, equal to 6.598 and 6.799%, respectively.

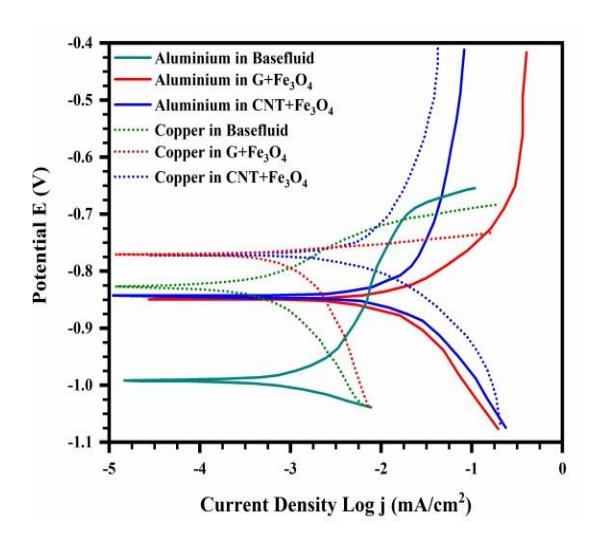


Fig. 6. Corrosion test for copper pipe and aluminum pipe.

3.6 Thermal conductivity measurements

Transfer plays an important role in many thermal applications such as solar collectors. Therefore, to better understand the process of heat transfer by changing the raw materials, the thermal conductivity of two nanofluids of graphene carbon nanoparticles/Fe₃O₄ magnetic nanoparticles and carbon nanotubes/Fe₃O₄ magnetic nanoparticles, for volume fractions of 0.2 to 0.1% and temperature range of 25 to 50 °C was measured. Fig. 7 shows the results of measuring the thermal conductivity of nanofluid graphene carbon nanoparticles/Fe₃O₄ magnetic nanoparticles water. As can be seen, with the increase of the volume fraction, the thermal conductivity of nanofluid increases, which is due to the conductivity of graphene particles and Fe₃O₄ magnetic nanoparticles. On the other hand, with the increase in temperature, the thermal conductivity of nanofluid increases, which can be caused by increasing the movement of particles and thus increasing the interaction between nano solid particles. The effect of adding carbon nanotubes to Fe₃O₄ magnetic nanoparticles on the thermal conductivity of nanofluid is shown in Fig. 7. As can be seen, as the volume fraction of carbon nanotubes increases, the thermal conductivity of the composite nanofluid increases, which can be due to the high thermal conductivity of carbon nanotubes. On the other hand, as the temperature increases, the thermal conductivity of the composite nanofluid increases.

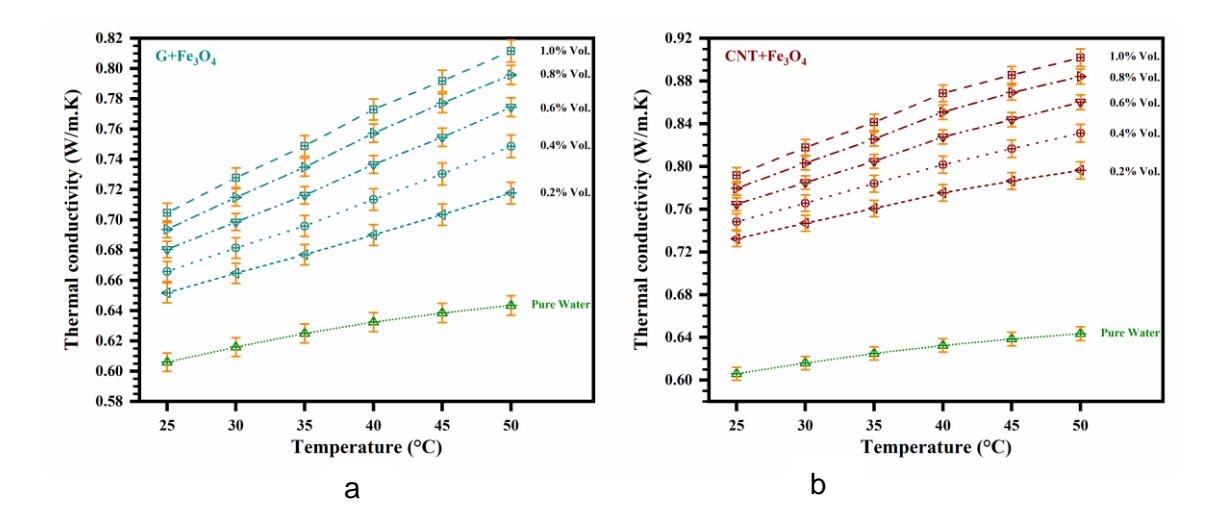


Fig. 7. Thermal conductivity for (a) graphene carbon nanoparticles/ Fe_3O_4 magnetic nanoparticles and (b) Carbon nanotube/ Fe_3O_4 magnetic nanoparticles.

Fig. 8 shows that carbon materials have high thermal conductivity. The increase in the thermal conductivity of the composite nanofluid containing positive graphene is 23.13%, compared to the thermal conductivity of water (at a volume fraction of 1% and a temperature of 50 °C). Also, the increase in the thermal conductivity of the composite nanofluid containing positive carbon nanotubes is 33.44%, compared to the thermal conductivity of water (at a volume fraction of 1% and a temperature of 50 °C).

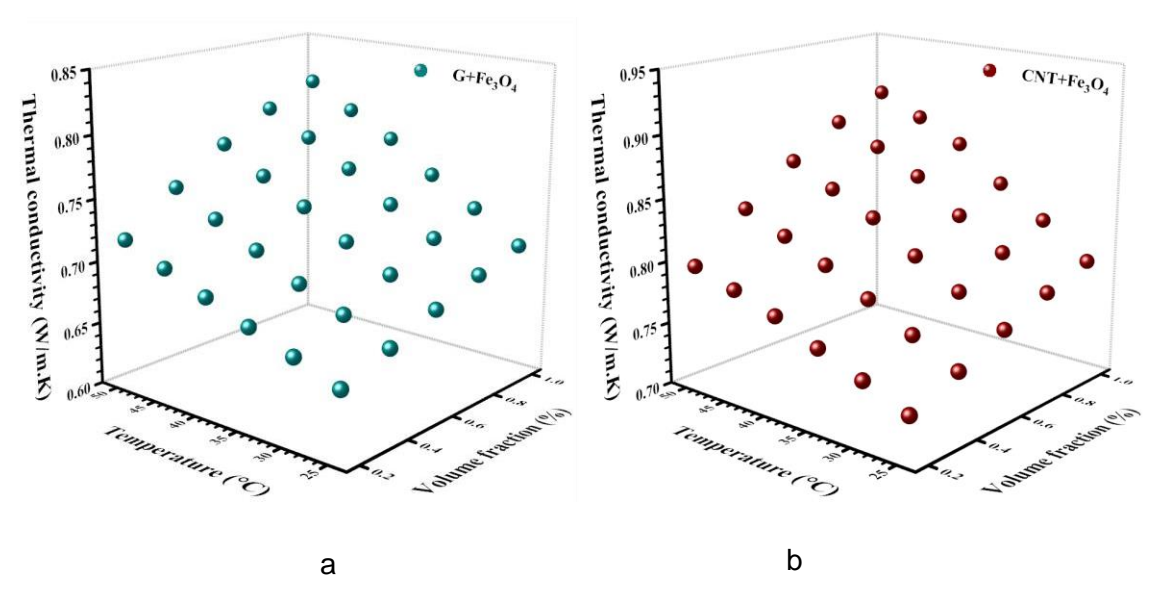


Fig. 8. 3D of thermal conductivity for (a) Graphene carbon nanoparticles/ Fe_3O_4 magnetic nanoparticles and (b) carbon nanotube/ Fe_3O_4 magnetic nanoparticles.

4. Conclusions

In this research, at first, the intermediate goal included the laboratory investigation of the corrosion of aluminum and copper tubes of flat plate solar collectors by two nanofluids, one magnetic nanofluid and the other magnetic nanofluid combined with carbon nanotubes. After that, the main goal was to reduce the corrosion in aluminum and copper pipes and, as a result, to reduce the maintenance costs of flat plate solar collectors in industries. In this research, the results after performing characterization tests, thermal-magnetic tests and corrosion tests are as follows:

The results of X-ray diffraction and Fourier transform infrared spectroscopy showed that the composite of magnetic nanoparticles/carbon nanotubes and magnetic nanoparticles/graphene nanoparticles contained the mentioned materials and the composition was well formed.

Also, the results of the scanning electron microscope showed that a good dispersion of Fe₃O₄ magnetic nanoparticles was formed in the graphene matrix, which were entangled and homogenized. The results of the thermal conductivity test showed that the increase in the thermal conductivity of the composite nanofluid containing positive graphene is 23.13%, compared to the thermal conductivity of water (at a volume fraction of 1% and a temperature of 50 °C). Also, the increase in the thermal conductivity of the composite nanofluid containing positive carbon nanotubes is 33.44%, compared to the thermal conductivity of water (at a volume fraction of 1% and a temperature of 50 °C). The results of the corrosion test of solar collector tubes showed that the corrosion potential for aluminum sample in base fluid, G+ Fe₃O₄ nanofluid and CNT+ Fe₃O₄ nanofluid is negative 0.991, 0.84 and 0.84, respectively. which shows the improvement of the corrosion resistance of solar collector aluminum tube in G+ Fe₃O₄ nanofluid and CNT+ Fe₃O₄ nanofluid samples compared to water, equal to 14.32 and 15.03%, respectively. Corrosion potential for copper sample in base fluid, G+Fe₃O₄ nanofluid and CNT+Fe₃O₄ nanofluid is negative 0.82679, 0.77224 and 0.77058 respectively. which shows the improvement of the corrosion resistance of solar collector copper tube in G+Fe₃O₄ nanofluid and CNT+Fe₃O₄ nanofluid samples compared to water, equal to 6.598 and 6.799%, respectively.

References

- [1] Leslie-Pelecky, D. L., & Rieke, R. D. Magnetic properties of nanostructured materials. Chemistry of materials, 8(8), 1770-1783. (1996).
- [2] Y. Hwang, J.K. Lee, C.H. Lee, Y.M. Jung, S.I. Cheong, Stability and thermal conductivity characteristics of nanofluids, Thermochim Acta, 455 (2007) 70–74.
- [3] Z. Said, A. A. Hachicha, S. Aberoumand, B. A. A. Yousef, E. T. Sayed, and E. Bellos, Recent advances on nanofluids for low to medium temperature solar collectors: energy, exergy, economic analysis and environmental impact, Prog. Energy Combust. Sci., 84 (2021) 100898.
- [4] Tan, D., Seng, A.K. Handbook for Solar photovoltaic (PV) systems. Energy Market Authority. Singapore. (2012).
- [5] Kalogirou, S. The potential of solar industrial process heat applications. Appl Energy. 337: 61-76 .(2003).

- [6] B. Ghorbani, K. B. Mahyari, M. Mehrpooya, and M.-H. Hamedi, Introducing a hybrid renewable energy system for production of power and fresh water using parabolic trough solar collectors and LNG cold energy recovery, Renew Energy, 148 (2020) 1227–1243.
- [7] El-Kassaby, M. M. Monthly and daily optimum tilt angle for south facing solar collectors; theoretical model, experimental and empirical correlations. Solar & wind technology, 5(6), 589-596. (1988).
- [8] A. M. Fadhil, J. M. Jalil, and G. A. Bilal, Experimental and numerical investigation of solar air collector with phase change material in column obstruction, J. Energy Storage, 79 (2024) 110066.
- [9] Villar, N. M., Lopez, J. C., Muñoz, F. D., García, E. R., & Andrés, A. C. Numerical 3-D heat flux simulations on flat plate solar collectors. Solar energy, 83(7), 1086-1092. (2009).
- [10] Otanicar, T. P., Phelan, P. E., Prasher, R. S., Rosengarten, G., & Taylor, R. A. Nanofluid-based direct absorption solar collector. Journal of renewable and sustainable energy, 2(3), 033102. (2010).
- [11] Tyagi, H., Phelan, P., & Prasher, R. Predicted efficiency of a low-temperature nanofluid-based direct absorption solar collector. Journal of solar energy engineering, 131(4). (2009).
- [12] Y. Xia, X. Lin, Y. Shu, and Z. Cheng, Enhanced thermal performance of a flat-plate solar collector inserted with porous media: A numerical simulation study, Therm. Sci. Eng. Prog., 44 (2023) 102063.
- [13] Malekahmadi, O., Kalanter, M., Nouri- Khezrabad, M. Effect of carbon nanotubes on the thermal conductivity enhancement of synthesized hydroxyapatite filled with water for dental applications experimental characterization and numerical study. Journal of Thermal Analysis and Calorimetry, 144, 2109-2126. (2021).
- [14] Q. Xiong, A. Hajjar, B. Alshuraiaan, M. Izadi, S. Altnji, and S. A. Shehzad, State-of-the-art review of nanofluids in solar collectors: A review based on the type of the dispersed nanoparticles, J. Clean. Prod., 310 (2021) 127528.
- [15] F. Shahzad., The effect of pressure gradient on MHD flow of a tri-hybrid Newtonian nanofluid in a circular channel, J. Magn. Magn. Mater., 568 (2023) 170320.
- [16] L. Qiu, N. Zhu, Y. Feng, E. E. Michaelides, G. Jing, et al., A review of recent advances in thermophysical properties at the nanoscale: From solid state to colloids, Phys Rep, 843 (2020) 1–81.
- [17] G. Singh, D. Bandhu Singh, S. Kumar, K. Bharti, and S. Chhabra, A review of inclusion of nanofluids on the attainment of different types of solar collectors, Mater Today Proc, 38 (2021) 153–159.
- [18] K. Rafique, Z. Mahmood, H. Alqahtani, and S. M. Eldin, Various nanoparticle shapes and quadratic velocity impacts on entropy generation and MHD flow over a stretching sheet with joule heating, Alexandria Eng. J., 71 (2023) 147–159.
- [19] N. Majeed, K. Sultan, and H. Anead, A Practical Study of The Thermal Performance of a Vacuum Tube For Solar Collector Using a Double -Sided Electronic Curtain With Nano-Fluid, Eng. Technol. J., 39 (2021) 1399–1408.
- [20] Sami Abed, Samir, Mehdi Sedighi3 and Abbas Ali Diwan, Influence Of Al_2O_3 Nano Additives On The Viscosity And Thermal Conductivity Of Double Distilled Water, Kufa Journal of Engineering, vol. 14, no. 2,. (2023). pp. 12-23,
- [21] Sun, B., Guo, Y., Yang, D., & Li, H. The effect of constant magnetic field on convective heat transfer of Fe_3O_4 /water magnetic nanofluid in horizontal circular tubes. Applied Thermal Engineering, 171, 114920. (2020).

- [22] Choi, S. U., & Eastman, J. A. Enhancing thermal conductivity of fluids with nanoparticles (No. ANL/MSD/CP-84938; CONF-951135-29). Argonne National Lab.(ANL), Argonne, IL (United States). (1995).
- [23] Batad, S. R., Andhare, D. D., Somvanshi, S. B., Kharat, P. B., More, S. D., & Jadhav, K. M. Preparation and characterisations of magnetic nanofluid of zinc ferrite for hyperthermia. Nanomaterials and Energy, 9(1), 8-13. (2020).
- [24] Hussain, S., Alam, M. M., Imran, M., Zouli, N., Aziz, A., Irshad, K., ... & Khan, A. Fe₃O₄ nanoparticles decorated multi-walled carbon nanotubes based magnetic nanofluid for heat transfer application. Materials Letters, 274, 128043. (2020).
- [25] Jang, S. P., & Choi, S. U. Role of Brownian motion in the enhanced thermal conductivity of nanofluids. Applied physics letters, 84(21), 4316-4318. (2004).
- [26] Raki, E., Afrand, M., & Abdollahi, A. Influence of magnetic field on boiling heat transfer coefficient of a magnetic nanofluid consisting of cobalt oxide and deionized water in nucleate regime: An experimental study. International Journal of Heat and Mass Transfer, 165, 120669. (2021).
- [27] Abdeen, D. H., Atieh, M. A., & Merzougui, B. Corrosion behaviour of 316L stainless steel in CNTs—water nanofluid: effect of temperature. Materials, 14(1), 119. (2020).